hexagon:2611.00800v1

HOLES AND ISLANDS OF VISIBLE POINTS ON THE TRIANGULAR LATTICE: MIDPOINT BOND GRAPHS AND PRIME-SIEVE BOUNDS

SABAH NOORI JIHAD

Abstract. For the induced complex on primitive integer pairs in a triangular lattice, we identify first homology with interior components of a half-scale midpoint bond graph. Its complementary planar dual has the visible-site graph as its line graph, giving a bijection between finite visible islands and bounded nonsingleton dual faces. In particular the hole density h is a local Euler-product term plus the island density b_0: $h = 3J_2 - 2J_3 - J_1 + b_0$, with $J_j = \prod_p (1 - j/p^2)$. Each odd prime produces a matching, two primes produce a small forest, and diameter exclusion bounds cycle birth. We refine the bounds by retaining the actual earlier prime sieve at each step. A computer-assisted certificate, including a nonnegative coverage recurrence for islands, yields $0.10917978 < h < 0.10923225$. A separate length-six finite-path CRT method gives $h > 0.10914952$, still below the island certificate, and an exact decomposition distinguishes old-component chords from cycles born among new cross-component bonds. Assuming the random-coprime nonpercolation theorem of Le Fourn–Liu–Martineau, the relative cycle increment of a new prime converges to a conditional connection probability. The planar correspondences, density existence, and numerical bounds do not require this probabilistic input.

1. Introduction

The visibility of an integer vector encodes the absence of a common prime divisor of its coordinates. Visible lattice sets have been studied through diffraction, pattern frequencies and arithmetic percolation [3, 4, 5, 6]. The density of visible points itself is classical; it does not directly describe the topology of an induced simplicial complex built on these points. Here we investigate the number of holes in a particular planar complex and connect them to the midpoints of edges in a coarser lattice. The broader motivation is quantitative topology of structured point sets: random simplicial complexes provide a contrasting framework (Kahle [2, Sections 1–2]), while arithmetic percolation studies connectivity in highly dependent visibility patterns. Our complexes are deterministic induced subcomplexes, not Linial–Meshulam complexes or independent percolation. The purpose is to identify which global topological counts admit exact local arithmetic descriptions.

Origin in the generative arithmetic fabric. The motivation comes from the author's *Generative Arithmetic Fabric* [1], a geometric workbench based on cumulative Cayley growth in $D_3 = \{(x, y, z) \in \mathbb{Z}^3 : x + y + z \equiv 0 \pmod 2\}$ with the twelve minimal root steps. Starting at the origin, successive applications of these steps give a graded lattice; arithmetic labels are read from the generated points rather than built into the growth rule. One graded triangular section is $(x, y) \mapsto (x, y, x + y)$ with $x, y \geq 0$ and shell index $x + y$: the minimal steps along the section are $(1, 0, 1), (0, 1, 1), (1, -1, 0)$ and their negatives. The coordinate gcd in this section is $\gcd(x, y)$. The earlier program motivated examining collisions of neighboring generated points at arithmetic midpoints. In this paper that idea becomes a precise two-scale model: the midpoint of an edge between two even points is tested for a common prime divisor, creating a bond if the midpoint is nonprimitive. Figure 1 illustrates the passage from graded growth to the planar readout; Figure 2 gives the midpoint rule. This citation records the provenance of the research question, not an assumption of any theorem from the earlier work.

The question arising in the author's earlier investigation is stated here independently: for the full primitive-vertex subcomplex K_k of the triangle $x, y \geq 0$, $x + y \leq k$ with triangular-lattice adjacency, does the limit $\lim_{k\to\infty} \beta_1(K_k)/k^2$ exist, and can it be bounded explicitly? The present paper supplies a proof and effective enclosures using an exact geometric reduction rather than assuming independence of nearby visible points. The main additional ingredients are the decomposition of the bond graph into prime matchings and a quantitative control of the resulting cycle rank. The construction should be distinguished from the theory of the size and existence of infinite clusters: the density of *components* counts each finite component once, not according to its

Date: 21 November 2026.

2020 *Mathematics Subject Classification.* Primary 11H06, 11N25; Secondary 05C10, 55N10, 52C07.

Key words and phrases. Visible lattice points, triangular lattice, Betti numbers, midpoint bond graph, prime sieves, Euler products, periodic approximation.

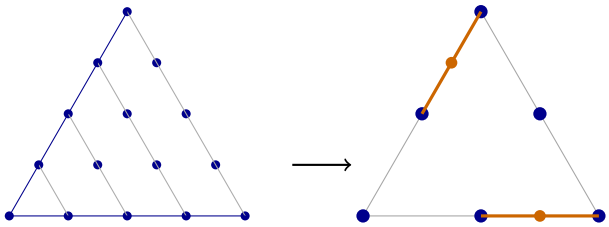


FIGURE 1. The generative origin of the planar construction. Successive shells give the triangular section; the even sublattice and selected nonprimitive midpoints give the coarse bond graph. Bonds are illustrated schematically, not exhaustively.

cardinality. No hypothesis on infinite components is needed for the existence and quantitative enclosures; the later prime-increment law uses a known random-model nonpercolation theorem.

Contributions and scope. The mathematical thesis is that global arithmetic absence (holes) equals a local Euler characteristic term plus finite islands of presence. The specific contributions for priority assessment are the exact boundary-preserving midpoint reduction and pointwise visible-island correspondence; the two Euler identities; prime matchings and two-prime forests; the diameter-sensitive and prime-stratified cycle-tail bounds and conditional asymptotic prime increment; and the certified numerical enclosure by complementary computations. The exact chord/nonchord decomposition and finite-path arithmetic certificate give an additional check of the sieve mechanism. The planar graph duality and inclusion–exclusion used in the expansion are standard tools. The face probabilities and cluster weights are explicit specializations of classical finite-pattern products; their use to bound this Betti density is specific to the present graph. Existence of a component density via a bounded-size approximation is already a standard consequence of pattern frequencies, and Cellarosi's Proposition 2.4 proves such an approximation for representatives of deep finite components on the cubical nearest-neighbor graph. We do not claim originality for that technique, Alexander duality, CRT, or Euler's formula. See Section 10 for the adjacency and observable distinctions. No claim of exhaustive priority is made.

2. The planar model and midpoint reduction

Work in $\Lambda = \mathbb{Z}^2$, endowed with the triangular-lattice adjacency given by

$$\mathcal{S}_+ = \{(1,0),(0,1),(1,-1)\}, \qquad \mathcal{S} = \mathcal{S}_+ \cup (-\mathcal{S}_+).$$

For $k \geq 1$, put $T_k = \{(x,y) \in \mathbb{Z}^2_{\geq 0} : x + y \leq k\}$, $n_k = |T_k| = (k+1)(k+2)/2$. Let $\mathcal{T}_k$ be its usual triangulation, in which each edge of difference in $\mathcal{S}$ is present and every elementary triangle is filled. Define

$$D_k = \{(x,y) \in T_k : \gcd(x,y) \neq 1\}, \qquad K_k = \mathcal{T}_k[T_k \setminus D_k],$$

with $\gcd(0,0) = 0$. Use integral simplicial homology throughout. A component of a graph contained in T_k is called interior if it has no vertex on $x = 0$, $y = 0$ or $x + y = k$. Denote its interior-component count by c_{int} and its total component count by c.

Lemma 2.1 (Planar component formula)**.** *For any deleted set $D \subset T_k$, the full induced complex on $T_k \setminus D$ has free first homology of rank $c_{\mathrm{int}}(D)$, where D carries the induced lattice adjacency.*

Proof. Let $X = |\mathcal{T}_k|$ be the closed triangular disc, $A = |\mathcal{T}_k[T_k \setminus D]|$ and $B_D = |\mathcal{T}_k[D]|$. Work in the one-point compactification S^2 of the ambient plane. The empty retained complex has $H_1 = 0$ and all deleted vertices form one boundary component, so suppose $A \neq \varnothing$.

Step 1 (deformation retraction). If $z \in X \setminus A$ has barycentric coordinates λ_v in a simplex, the sum $b(z) = \sum_{v \in D} \lambda_v$ is positive because A is full. Define

$$R(z) = \sum_{v \in D} \frac{\lambda_v}{b(z)} v, \qquad H(z,t) = (1-t)z + tR(z).$$

All expressions use the vertices of the containing simplex. The restrictions agree on common faces, and the homotopy stays in that simplex with positive deleted weight; it fixes B_D pointwise. This gives a strong deformation retraction onto B_D and also preserves the boundary when restricted to $\partial X \setminus A$. Its components are exactly the

graph components of the deleted vertices: every simplex connects its vertices by edges. This includes the case $D = \varnothing$, when $X \setminus A$ is empty.

Step 2 (exterior and boundary). A component of $X \setminus A$ meets ∂X exactly when its retracted deleted component contains a boundary vertex. Each such component connects to the single exterior region $S^2 \setminus X$: any point of $\partial X \setminus A$ has a small neighborhood disjoint from the closed set A, containing exterior points. An interior component cannot connect to the exterior, since a path leaving X must first meet ∂X without meeting A. No two interior components can join via the exterior for the same reason. These arguments apply to path components (the open complement in S^2 is locally path connected). Thus $S^2 \setminus A$ has precisely $1 + c_{\mathrm{int}}(D)$ components. All three sides, including the corners, are counted as boundary.

Step 3 (duality and integral homology). The nonempty finite polyhedron A is compact and locally contractible, a proper subset of S^2. Alexander duality, Hatcher [7, Corollary 3.45], gives $\widetilde{H}^1(A;\mathbb{Z}) \cong \widetilde{H}_0(S^2 \setminus A;\mathbb{Z}) \cong \mathbb{Z}^{c_{\mathrm{int}}(D)}$. To see that $H_1(A;\mathbb{Z})$ has no torsion, repeatedly remove a triangle together with a free edge: whenever a triangle remains, the union of remaining closed triangles is a finite planar union with an exposed side incident to exactly one triangle. Such a side exists, for example by taking a generic ray from an interior point to infinity and the last triangle side crossed. Each removal is an elementary simplicial collapse. The resulting finite graph has free integral first homology. By the universal coefficient theorem (with H_0 free), the rank of H_1 is the rank of H^1. No connectedness of A was required. This proves the claim. □

Definition 2.2 (Midpoint bond graph)**.** On the coarse lattice $\mathbb{Z}^2$, let G have the edge $\{u, u+s\}$, $s \in \mathcal{S}_+$, if and only if

$$\gcd(2u_1 + s_1, 2u_2 + s_2) > 1. \tag{1}$$

The point $2u + s$ is the midpoint of the edge joining $2u$ to $2(u + s)$ in the original lattice. Write $G_m = G[T_m]$ for the induced coarse graph. Isolated coarse vertices are included. We also call this the collision graph, in the terminology of the motivating fabric; this name describes midpoint incidence, not a physical process.

Theorem 2.3 (Exact midpoint reduction)**.** *For each $m \geq 1$, the connected components of the deleted graph on D_{2m} correspond bijectively to those of G_m. Under the correspondence, touching the boundary is preserved. In particular,*

$$H_1(K_{2m};\mathbb{Z}) \cong \mathbb{Z}^{c_{\mathrm{int}}(G_m)}, \qquad \beta_1(K_{2m}) = c_{\mathrm{int}}(G_m). \tag{2}$$

Proof. All vertices of $2\mathbb{Z}^2 \cap T_{2m}$ are deleted, including the origin. We give the geometric details of the correspondence.

Midpoint classification. The triangulation obtained by scaling $\mathcal{T}_m$ by two has vertex set $2T_m$. Subdivide each of its triangles by joining the midpoints of its three sides. The resulting triangulation is exactly $\mathcal{T}_{2m}$: the four subtriangles are elementary lattice triangles of the original orientation or its reverse. For the three nonzero parity classes, representatives $(2a+1, 2b)$, $(2a, 2b+1)$, $(2a+1, 2b+1)$ have unique pairs of coarse endpoints, respectively

$$\begin{array}{ll} (2a, 2b), & (2a+2, 2b), \\ (2a, 2b), & (2a, 2b+2), \\ (2a+2, 2b), & (2a, 2b+2). \end{array}$$

If the midpoint lies in T_{2m}, these endpoints lie there too: for the first two classes its sum of coordinates is odd and at most $2m - 1$; for the last class both endpoint sums equal the midpoint sum. These are its only even neighbors, since the six lattice directions contain exactly two directions of the relevant parity. There are no fine edges between distinct even vertices. The subdivision also classifies each fine edge between two midpoints: it is an interior side of one subdivided coarse triangle. The two corresponding coarse sides share a coarse vertex.

Preservation of components. Whenever two deleted midpoints are adjacent, their common even neighbor is deleted as well. Remove all midpoint–midpoint edges simultaneously; each removed edge has an alternative path of length two consisting entirely of retained edges of the deleted graph. Replacing every removed edge on any original path gives a walk in the reduced graph, and the reverse implication holds by inclusion. Every remaining deleted midpoint has degree two and occurs precisely when its coarse edge is active by (1). Thus the remaining graph is exactly the edge subdivision of G_m, with isolated coarse vertices included. Suppressing each degree-two midpoint preserves the components in both directions.

Preservation of the boundary. For each of the three defining affine inequalities of the triangle, an average of two nonnegative slacks is zero exactly when both slacks vanish. Hence a deleted midpoint lies on a given side if and only if both coarse endpoints lie on that side. An even vertex on the boundary corresponds to a coarse boundary vertex. The component bijection therefore preserves meeting the boundary, including the corners. Lemma 2.1 now gives (2). This is a correspondence of components; it does not assert that the full deleted graph and G_m

have equal cycle ranks. The same local midpoint classification and path replacement hold on the entire plane whenever all even sites are deleted, with arbitrary remaining deletions. The subdivision associates finitely many midpoints to each coarse vertex and every coarse vertex is itself a deleted site. Thus corresponding components are finite simultaneously. This extension will be used only in the auxiliary random-residue model. □

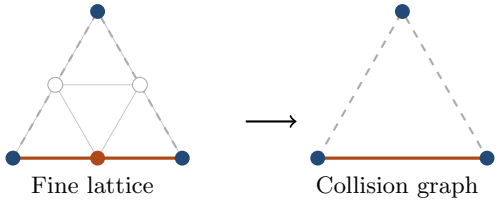


FIGURE 2. Schematic reduction of a coarse triangle. Blue vertices are always deleted even points. An orange midpoint is deleted and activates its coarse edge; unfilled midpoints do not. For an actual example, add $(2, 6)$ to the three displayed fine vertices: the horizontal midpoint $(3, 6)$ is nonprimitive, whereas $(2, 7)$ and $(3, 7)$ are primitive.

Lemma 2.4 (Odd–even equality)**.** *For every $m \geq 1$, $\beta_1(K_{2m-1}) = \beta_1(K_{2m})$.*

Proof. A new primitive vertex on $x + y = 2m$ has both coordinates odd. Its neighbors on that outer line are even and deleted. Its only possible retained neighbors are the two vertices one step inward, which are adjacent if both are retained. Hence each new vertex attaches along an empty, singleton or one-edge link; in the latter two cases its cone collapses back to the link. In the empty case it is an isolated new vertex. These operations do not change first homology. The two corner vertices on the new side are nonprimitive (their nonzero coordinate is $2m$). The new primitive vertices are pairwise nonadjacent, so their links are already in K_{2m-1} and the collapses can be performed independently, including when $m = 1$. □

3. Periodic prime sieves and the existence of the limit

The main limiting quantities below are normalized per fine vertex: h counts holes, h_P coarse components at cutoff P, ρ, ρ_P cycle ranks, e, e_P bonds, and $\delta_P = e - e_P$ omitted bonds. The island density b_0 counts visible components, whereas B_L bounds the conditional fraction of cycle-eligible new bonds.

For real $P \geq 3$ define $\mathcal{P}_P = \{p : 3 \leq p \leq P,\ p \text{ prime}\}$, $M_P = \prod_{p \in \mathcal{P}_P} p$. Let $G^{(P)}$ have all coarse vertices and only bonds in (1) witnessed by some $p \in \mathcal{P}_P$. No midpoint has both coordinates even, so the union over all odd primes is G. The truncated graph has period $M_P\mathbb{Z}^2$.

Write $E_P(m)$ and $E(m)$ for the edge counts of $G^{(P)}[T_m]$ and G_m. Our densities are normalized by n_{2m} (fine-lattice points), not n_m (coarse-lattice points). In particular $n_m/n_{2m} \to 1/4$. Put

$$e_P = \frac{3}{4}\left(1 - \prod_{3 \leq p \leq P}(1 - p^{-2})\right), \qquad e = \frac{3}{4} - \frac{6}{\pi^2}, \qquad \delta_P = e - e_P. \tag{3}$$

In all products, p denotes a prime unless otherwise stated. The CRT gives $\lim_m E_P(m)/n_{2m} = e_P$: for each of the three orientations, $2u + s \equiv 0 \pmod{p}$ is a single residue class of u modulo p, independent across primes. For the full sieve, the tail is controlled by counting points divisible by $p > P$. Since midpoint coordinates in T_{2m} are between 0 and $2m$, and the midpoint is never the origin, all its prime divisors are at most $2m$. For such p, the number of multiples of p in the triangle is $O(m^2/p^2 + m/p + 1)$ uniformly. Summing over integers $p > P$ yields an upper bound $O(m^2/P + m \log m + m)$ for the omitted set. Periodic densities therefore converge to the full density. By $\prod_p(1 - p^{-2}) = 6/\pi^2$ we obtain the second formula of (3) and, more precisely,

$$\lim_m \frac{E(m) - E_P(m)}{n_{2m}} = \delta_P \leq \frac{3}{4}\sum_{p>P} p^{-2}. \tag{4}$$

The same argument proves existence of every finite local pattern density of bonds: the difference between full and truncated pattern events is bounded by the union of the finitely many translated omitted-bond events. For fixed offsets the counting box expands by only a fixed amount; a nonzero midpoint has maximum absolute coordinate $O(m)$ and the midpoint cannot be zero because its parity is nonzero. Residue counts in a fixed-period triangle

are $n_m/M^2 + O_M(m)$ per class, including axes and corners. Thus the stated CRT probabilities apply to triangle averages, not merely box averages. This is an elementary instance of the established pattern-frequency theory [4].

Lemma 3.1 (Periodic component density)**.** *In the quotient graph of $G^{(P)}$ by $M_P\mathbb{Z}^2$, let F_P be the number of components whose lifts to $\mathbb{Z}^2$ are finite. Then*

$$h_P := \lim_{m\to\infty} \frac{c(G^{(P)}[T_m])}{n_{2m}} = \frac{F_P}{4M_P^2}.$$

Proof. A component in the finite quotient lifts to finite components precisely when all closed walks in it have zero displacement in $M_P\mathbb{Z}^2$. In that case each lift contains one copy of every quotient vertex of that component, and exactly one translate per period cell of any chosen representative. Each finite lifted component accordingly contributes one per M_P^2 coarse vertices, up to a boundary error $O_P(m)$ in T_m. There are finitely many quotient components, hence their finite lifts have uniformly bounded sizes for fixed P. A restriction of an infinite lifted component to T_m can only have components meeting the boundary, since a path to infinity must leave T_m by a nearest-neighbor edge. Their number is $O(m)$ in total. Dividing by n_{2m} proves the formula. The displacement criterion also provides an exact finite algorithm: traverse each quotient component with integer lifted coordinates; inconsistency along a previously visited vertex detects nonzero displacement. □

Theorem 3.2 (Existence and effective approximation of the hole density)**.** *The limit*

$$h = \lim_{k\to\infty} \frac{\beta_1(K_k)}{n_k} \tag{5}$$

exists. The sequence h_P decreases to h and obeys

$$h_P - \delta_P \le h \le h_P, \qquad \lim_{k\to\infty} \frac{\beta_1(K_k)}{k^2} = \frac{h}{2}. \tag{6}$$

In particular the constant can be approximated to arbitrary prescribed absolute accuracy with finite exact quotient counts and a prime-sieve tail bound.

Proof. Adding a single bond decreases the number of components by either zero or one. For every m,

$$c(G^{(P)}[T_m]) - (E(m) - E_P(m)) \le c(G_m) \le c(G^{(P)}[T_m]).$$

The difference between $c(G_m)$ and $c_{\mathrm{int}}(G_m)$ is at most the number of boundary vertices, $O(m)$. Divide by n_{2m} and apply Theorem 2.3, Lemma 3.1 and (4). The limsup and liminf differ by at most δ_P for each P, and $\delta_P \to 0$. Monotonicity of the truncated component counts gives monotonicity of h_P; the bounds give its limit. Lemma 2.4 extends the even subsequence limit to all k. Finally $n_k/k^2 \to 1/2$. □

Corollary 3.3 (Cycle-density identity)**.** *Let $r(H) = |E(H)| - |V(H)| + c(H)$ be the cycle rank of a finite graph. The limits $\rho = \lim_m r(G_m)/n_{2m}$ and $\rho_P = \lim_m r(G^{(P)}[T_m])/n_{2m}$ exist and*

$$h = \frac{6}{\pi^2} - \frac{1}{2} + \rho, \qquad \rho_P = e_P - \frac{1}{4} + h_P, \qquad 0 \le \rho - \rho_P \le \delta_P. \tag{7}$$

In particular $h > 0$.

Proof. Use the graph identity for cycle rank, $n_m/n_{2m} \to 1/4$, and (3)–(5). Adding an edge increases cycle rank by at most one and never decreases it. The lower bound $6/\pi^2 - 1/2 > 0$ follows from $\rho \ge 0$. □

4. Planar duality and elementary faces

Put $Q_j = \prod_{p\ge3}(1 - j/p^2)$ for $0 \le j \le 5$. The complementary dual graph has one vertex per elementary triangle and joins adjacent triangles exactly when their shared coarse bond is absent. In T_m include an exterior dual vertex on S^2 and connect across absent boundary sides. The components of this dual graph are the faces of G_m: deleting a primal edge merges its incident regions if distinct, and otherwise leaves them unchanged. Thus its component count minus one is the cycle rank, by Euler's planar formula. This construction works for disconnected graphs, isolated primal vertices, bridges and non-simple boundary walks. The infinite locally finite construction has the same face incidence; a bounded face corresponds to a finite dual component.

Proposition 4.1 (Elementary face probabilities)**.** *The probability of an elementary triangular bounded face is $t = 1 - 3Q_1 + 3Q_2 - Q_3$. That of a two-triangle rhombic bounded face is $b = Q_1 - 4Q_2 + 6Q_3 - 4Q_4 + Q_5$. Hence $\rho \ge t/2 + 3b/4$.*

Proof. The three midpoint offsets of the triangle are $\mathbf{e}_1, \mathbf{e}_2, \mathbf{e}_1+\mathbf{e}_2$, with $\mathbf{e}_1=(1,0), \mathbf{e}_2=(0,1)$. Require all three active. For the rhombus with vertices $0, \mathbf{e}_1, \mathbf{e}_2, \mathbf{e}_1+\mathbf{e}_2$, require its four outer midpoints $\mathbf{e}_1, \mathbf{e}_2, 2\mathbf{e}_1+\mathbf{e}_2, \mathbf{e}_1+2\mathbf{e}_2$ active and its diagonal midpoint $\mathbf{e}_1+\mathbf{e}_2$ absent. These offsets are distinct modulo every odd prime in each test; CRT and inclusion–exclusion give the formulas. They count actual faces, hence are disjoint as face interiors; there are two triangles and three candidate rhombi per coarse vertex asymptotically. Fine normalization gives the result. □

For general finite triangle sets A, the event that A is exactly a dual component requires active boundary sides and a connected complementary dual graph on A. Summing exact internal-edge configurations over normalized shapes of size at most K gives a lower estimate Φ_K for ρ; larger dual components consume at least $K+1$ triangles each, so $0 \le \rho - \Phi_K \le 1/[2(K+1)]$. The supplement gives the full finite-pattern formula and certificate. This count permits dangling active edges inside a face, rather than assuming all its interior sides are absent.

5. Holes and islands: the complementary correspondence

Call a finite component of the primitive-site graph an island. In an even finite triangle we call a visible component interior if it avoids the three boundary sides. The deleted-site and visible-site components are different objects. We now show why the nontriangular bounded faces of the midpoint graph encode the latter.

Theorem 5.1 (Pointwise island–face correspondence)**.** *Every bounded face of the infinite midpoint graph other than the interior of a single elementary triangle corresponds to exactly one finite visible-site component, and conversely. For G_m, bounded faces consisting of at least two dual triangle vertices correspond bijectively to interior components of the visible graph on T_{2m}. In both cases the component consists of the visible midpoints of absent coarse sides between the triangles in that dual component.*

Proof. Use the mid-edge subdivision of Theorem 2.3. All even vertices are deleted, so every visible site is the midpoint of exactly one absent coarse side. A fine edge joining two such midpoints lies in a single subdivided coarse triangle, and conversely any two distinct sides of a coarse triangle have adjacent midpoints. Thus visible-site adjacency agrees precisely with edge incidence in the dual subgraph on triangles: the visible graph in the full plane is the line graph of the complementary dual graph (isolated dual vertices contribute no line-graph vertices). For a connected graph containing an edge, its line graph is connected; a finite component with at least one edge has a nonempty finite connected line graph and an infinite component of this locally finite dual graph has infinitely many edges. The dual component with no edges is an isolated triangle whose three sides are all active. Planar duality from Section 4 identifies the finite dual components with bounded faces. For a finite triangle the exterior vertex may identify boundary edges that are not mutually adjacent in the visible graph, so apply the line-graph statement only to dual components not containing the exterior. A visible component meets the boundary exactly when it contains a midpoint of an absent boundary side. Such a side is incident to the exterior dual vertex. Conversely any chain of dual edges from an interior triangle to the exterior gives a chain of midpoint adjacencies until the first boundary side. This proves the finite assertion and handles isolated visible sites, bridges, and annular faces without requiring simple cycles. □

Write $J_j = \prod_p (1 - j/p^2)$ for $j = 1, 2, 3$, and let

$$b_0 = \lim_{k\to\infty} \frac{\beta_0(K_k)}{n_k}, \qquad \bar{\chi} = J_1 - 3J_2 + 2J_3.$$

The limit is justified in the next proof; the same density is obtained by counting only interior visible components. The normalized density b_0 counts islands, not their vertices.

Theorem 5.2 (Two Euler identities)**.** *The island density exists and*

$$h = -\bar{\chi} + b_0 = 3J_2 - 2J_3 - J_1 + b_0, \qquad \rho = \tfrac{1}{2}(1 - 3Q_1 + 3Q_2 - Q_3) + b_0. \tag{8}$$

Proof. The local number of retained vertices, edges and filled elementary triangles per fine vertex tends respectively to $J_1, 3J_2, 2J_3$. Indeed each edge or triangle has distinct vertex residues modulo every prime: differences are minimal directions with a coordinate ± 1. CRT and the prime-tail estimate of Section 3 give the three products, treating the origin separately as one point. Boundary counts of the potential edges and triangles are $O(k)$. The finite planar complex has $H_2 = 0$ by the collapse in Lemma 2.1; hence $\beta_1 = \beta_0 - \chi$ even if disconnected. Since h exists, the limit for β_0/n_k is $h + \bar{\chi}$. Removing components meeting the boundary changes at most $3k$ counts. Every interior component is a finite component of the infinite visible graph, and a finite component fully contained in the interior is counted. Its density follows equivalently by fixed-size truncation, with components larger than

L contributing at most $1/(L+1)$. This proves the first formula. Since $J_1 = 3Q_1/4$, $J_2 = Q_2/2$, $J_3 = Q_3/4$, comparison with (7) proves the second. Alternatively Theorem 5.1 proves it directly: singleton dual components have density $(1 - 3Q_1 + 3Q_2 - Q_3)/2$ in fine normalization and all remaining bounded faces count islands. □

Remark 5.3 (Short-range exclusion and the hexagon). An elementary isolated dual triangle requires three active sides; a two-triangle face requires four active sides and one absent diagonal. Compare their probabilities t and b from Proposition 4.1 to the artificial independent-edge reference p_e^3 and $p_e^4(1-p_e)$, where $p_e = 1 - 8/\pi^2$. The reference is not a model of the arithmetic dependencies. An instructive opposite phenomenon occurs for the six-triangle hexagon centered at a coarse vertex: the six boundary midpoint offsets, sums of consecutive nearest-neighbor directions, fall into just two classes $(1,1)$ and $(-1,-1)$ modulo 3. The six spoke offsets are the six distinct nonzero root residues, disjoint from these two classes. Thus a single residue choice for $p = 3$ can activate three alternating boundary bonds at once without activating any spoke. The site-cluster expansion below also captures this geometry as a six-midpoint ring. The finite cutoff $R = 10000$ gives approximate ratios to the full-density independent reference of 0.316 (triangle), 0.127 (rhombus), and 3.922 (isolated-center hexagon), calculated from the same finite pattern products. These ratios are descriptive, not certified limiting constants. The enhanced size-six contribution is a local arithmetic correlation; no conclusion about the existence of infinite clusters follows from comparison with independent bonds.

6. Prime matchings and an improved tail estimate

The decomposition into prime sieves has a special property not visible in the one-point visibility density.

Proposition 6.1 (Matching and two-prime forest)**.** *For any odd prime p, the edges witnessed by p form a matching. For any two distinct odd primes p, q, their union is a forest, all of whose components have at most four vertices. If $p, q \geq 5$, each component has at most three vertices; a component with four vertices can occur only if one of the primes is 3.*

Proof. At a vertex u, the six incident midpoint residues are $2u + s$, $s \in \mathcal{S}$. They are distinct modulo any odd prime, because no difference of distinct directions has all coordinates divisible by such a prime. Thus at most one incident edge is witnessed by p, establishing the matching property.

Assume $q \geq 5$ after possibly relabelling. Along a simple path, label each edge by any one of its witnesses in $\{p, q\}$. Consecutive labels differ. A subpath of three edges with labels q, p, q is impossible. If its successive coarse directions are $d_1, d_2, d_3 \in \mathcal{S}$, the difference of the first and third fine midpoints is $d_1 + 2d_2 + d_3$. Each coordinate has magnitude at most 4, and this difference is nonzero because distinct coarse edges have distinct midpoints. It cannot belong to $q\mathbb{Z}^2$. An alternating path of length four would contain q, p, q; an alternating cycle likewise would contain it (a cycle is necessarily even because labels alternate). Thus there are no cycles or paths of length four. Since the degree is at most two, the components are paths of at most three edges, including isolated vertices. If both primes are at least 5, interchange their roles: the pattern p, q, p is also impossible by the same nonzero displacement bound. Every three-edge alternating path has one of these two patterns. Hence all paths have at most two edges, giving the asserted sharper bound. An edge witnessed by both primes is an isolated two-vertex component of the two-prime graph, since each prime already occupies both endpoints. A multiply witnessed edge cannot create an exception: at a vertex shared with another edge, it could not share either prime, by the matching property. In particular any choice of witnesses on a simple path is alternating. □

At the first level the following conditional probability has a closed form:

$$B = 1 - 2\prod_{p \geq 3}(1 - 5/(p^2 - 1)) < 1. \tag{9}$$

Indeed, given a central absent bond, the five other incident offsets at either endpoint are distinct modulo every odd prime and avoid the central residue. The conditional isolation probability at one endpoint is the product in (9). Both endpoints cannot be isolated: the eleven incident midpoint offsets together cover all nine classes modulo 3. In the full sieve, the probability that both endpoints are nonisolated is therefore B. The product is positive by convergence of $\sum p^{-2}$. The size-sensitive theorem below includes this first-level bound.

6.1. Diameter exclusion and a hierarchy of cycle bounds.

For an integer $L \geq 1$, let B_L denote the conditional spatial probability of the following event for the potential coarse edge $a = \{u, v\}$, given that a is absent from G:

$$\mathcal{E}_L(a) = \{C(u) = C(v)\} \cup \{|C(u)| > L,\ |C(v)| > L\}, \tag{10}$$

where $C(w)$ denotes the component of w in the graph, with infinite size allowed. Equivalently, the event fails if an endpoint belongs to a component of at most L vertices which does not contain the other endpoint. This equivalent form is a finite local test: explore each endpoint out to graph distance $L-1$ in the underlying lattice and inspect all edges incident to the explored neighborhood. It detects every component of at most L vertices together with its closed boundary. Thus the conditional probability exists by the finite-pattern argument in Section 3. The event is increasing under edge addition with a held absent, and $B_{L+1} \le B_L$. Symmetry makes it independent of edge orientation. In particular $B_1 = B$ of (9).

Lemma 6.2 (Diameter exclusion)**.** *Let C be a component before a new prime q is added. If C has ℓ^∞ diameter at most D and $q > 2D+2$, at most one distinct q-witnessed edge can touch C.*

Proof. Choose endpoints u_1, u_2 in C of two such edges and write their fine midpoints as $2u_i + s_i$, $s_i \in \mathcal{S}$. Their difference has infinity norm at most $2D+2$, is nonzero by uniqueness of edge midpoints, and belongs to $q\mathbb{Z}^2$. This is impossible under the stated strict inequality. □

Theorem 6.3 (Size-sensitive cycle tail)**.** *For every positive integer L and real $P \ge \max(3, 2L)$,*

$$0 \le \rho - \rho_P \le B_L \delta_P, \qquad h \le \frac{6}{\pi^2} - \frac{1}{2} + \rho_P + B_L \delta_P.$$

Proof. First work in the finite induced graph on T_m and add a prime $q > P$ to an old finite prime sieve S. Contract each connected component of the old graph to one vertex and keep the genuinely new edges, including loops and parallel edges. The cycle-rank increment is the cycle rank of this multigraph: the identity $r = E - V + c$ gives this directly before and after contraction. If an old component has at most L vertices, its diameter is at most $L-1$. Lemma 6.2 shows that at most one new edge touches it. If that edge is not a loop, it is a bridge of the contracted graph and contributes no cycle rank. If it is a loop, its endpoints were in the same old component; this possibility must be counted. Removing all such bridges leaves only edges joining two large components or edges whose endpoints were in one old component. The rank increment is at most their number, so every eligible edge satisfies $\mathcal{E}_L$ in the old graph. For $L = 2$ a genuinely new loop inside a small component is impossible, since a connected two-vertex component already contains its only potential edge. For $L \ge 3$ this exception cannot be omitted.

For fixed S, q, L, finite-boundary effects in the local test are $O_L(m)$ vertices. Conditional on the candidate edge being absent in S, the residue of the coarse translation modulo each $p \in S$ is uniform over the $p^2 - 1$ classes avoiding that edge. Additional prime residues conditioned to avoid the edge have independent CRT distributions. They can only increase $\mathcal{E}_L$. Consequently the conditional probability for S is bounded by B_L, obtained as the limit of the full conditional finite-pattern frequencies. Activation by q is independent of the old residues. Taking the spatial limit gives the increment bound B_L times the genuinely new edge density. Sum this inequality over $P < q \le R$ and let $R \to \infty$ using (7) and (4). □

This result controls additional cycles without a Bernoulli percolation assumption, and holds even if the deterministic graph has infinite components. The chord exception is essential: excluding every small component without distinguishing loops would not prove the theorem.

6.2. **A prime-stratified bound.** For a finite sieve S of odd primes, let $b_L(S)$ denote the conditional probability of $\mathcal{E}_L$ in that sieve, given absence of the central bond. This probability is calculated with the independent, uniform residue choices for the primes in S, which agree with spatial frequencies by CRT. Its full-sieve counterpart is B_L; coupling the residues prime by prime, all conditional graphs have the central bond absent, so $b_L(S) \le B_L$.

Theorem 6.4 (Stratified sieve-memory bound)**.** *For a prime q let $S_{<q} = \{p : 3 \le p < q\}$, and choose integers $L_q \ge 1$ with $2L_q < q$. Then*

$$0 \le \Delta\rho_q \le b_{L_q}(S_{<q})\Delta e_q, \qquad \Delta e_q = \frac{3}{4q^2} \prod_{3 \le p < q} (1 - p^{-2}).$$

In particular for a finite cutoff $U > P$, and a fixed L with $2L < U$,

$$\rho - \rho_P \le \sum_{P < q \le U} b_{L_q}(S_{<q})\Delta e_q + B_L \delta_U.$$

Proof. Use precisely the contraction in Theorem 6.3, retaining the old graph rather than replacing it by the full graph. Each new edge eligible to contribute satisfies $\mathcal{E}_{L_q}$ in the old graph. The CRT makes the event of activation by q independent of the finite old-sieve event; density of eligible new edges is therefore $b_{L_q}(S_{<q})\Delta e_q$,

using the three orientations and normalization from (3). Summing the finite increment inequalities and applying the full-sieve tail bound after U proves the second inequality. Here $\Delta\rho_q = \rho_q - \rho_{q^-}$ and $\Delta e_q = e_q - e_{q^-}$, with q^- denoting the sieve over primes strictly below q. □

Proposition 6.5 (Exact chord criterion)**.** *In an old periodic graph all of whose lifted components are finite, suppose every absent bond joining distinct lifted components has at least one endpoint in an old component of infinity diameter D with $2D + 2 < q$. Then every cycle added by q is attributable to an old-component chord, and the rank increment equals the number of genuinely new chords in the density limit. If there are C absent chords in a period cell of M^2 coarse vertices (counting each of the three positive orientations), then $\Delta\rho_q = C/(4M^2q^2)$.*

Proof. After contraction each cross-component new edge has an endpoint touched by no other new edge, by Lemma 6.2; hence it is a bridge. Each loop contributes one to rank, independently of other loops, by $r = E - V + c$. Since the finitely many quotient components have finite lifts, their diameters are uniformly bounded, so passing from the full graph to large triangles changes the chord and bridge tests only near their boundaries. Old chord membership is periodic, and CRT gives a $1/q^2$ fraction of these absent midpoints activated by q. Normalize by $4M^2$. □

7. A conditional cycle-increment law

For an odd prime q, write ρ_{q^-} and e_{q^-} for the densities with all odd primes strictly less than q, and put $\Delta\rho_q = \rho_q - \rho_{q^-}$ and $\Delta e_q = e_q - e_{q^-}$. Let θ be the probability, in the independent-residue model on all odd primes, that the endpoints of a potential bond are connected conditional on that bond being absent. This is a countable product probability; it is the increasing limit of the corresponding connection events in finite windows, not a claim about any exceptional deterministic origin.

Theorem 7.1 (Asymptotic prime increment, conditional on random nonpercolation)**.** *Assume the almost-sure nonpercolation statement for the nonvisible set in the triangular random coprime coloring (the statement of* [5, Theorem 1.7]*). For primes $q \to \infty$,*

$$\frac{\Delta\rho_q}{\Delta e_q} \longrightarrow \theta, \qquad q^2\Delta\rho_q \longrightarrow \frac{6}{\pi^2}\theta, \qquad \frac{\rho - \rho_P}{\delta_P} \longrightarrow \theta \quad (P \to \infty).$$

Proof. Condition on the fine residue class of 2 being zero in the stationary random-coprime model of Le Fourn–Liu–Martineau [5, Theorem 1.7]; this has probability $1/4$, so their almost-sure absence of an infinite nonvisible cluster still holds. Given that class, the remaining odd-prime residues are independent and uniform, exactly the model of our coarse bond graph. The full-plane extension in Theorem 2.3 applies to these arbitrary deleted sets and proves that all its components are finite almost surely. The additional conditioning that the central bond is absent has positive probability Q_1. Therefore the decreasing events $\mathcal{E}_L$ of (10) have limiting probability θ: two different finite components eventually fail the joint size test. By Theorem 6.3's one-prime argument, for each fixed L and all primes $q > 2L$, $\Delta\rho_q/\Delta e_q \le B_L$. For the reverse inequality, fix a finite window and a finite prime cutoff R. Every genuinely new bond with endpoints already connected by a path in that old window contributes one loop after contracting old components. The intervening primes between R and q only add bonds and cannot destroy the path. Adding each loop raises E by one without changing V or c, so these loops add individually to rank, even if they meet other new edges. For $q > R$, conditional on absence from all primes less than q, the old primes up to R have exactly their distributions conditioned on central absence, independently of activation by q. Thus the ratio is at least the probability of that finite connection test. Boundary loss of these fixed-window tests is $O_{R,\mathrm{window}}(m)$ for each fixed window and cutoff. Increase both the cutoff and the window to exhaust all finite paths: continuity from below in the product measure gives lower limit at least θ. Now let L increase for the upper limit. This proves the first limit. CRT gives $\Delta e_q = (3/4)q^{-2}\prod_{3\le p<q}(1 - p^{-2})$, proving the second. Finally the tail ratio is a weighted average of the increment ratios, with positive weights Δe_q summing to δ_P, so it has the same limit. □

This theorem concerns the asymptotic cycle production of an individual prime and the entire sieve tail, using a known probabilistic nonpercolation theorem rather than assuming independent bonds. No deterministic nonpercolation claim is needed. Positivity of θ follows, for example, from a two-edge detour around an elementary triangle with two different prime witnesses and the central bond absent (CRT and a positive remaining avoidance product).

Corollary 7.2 (Rate of periodic approximation, under the same hypothesis)**.** *As* $P \to \infty$,

$$h_P - h = (1 - \theta + o(1))\delta_P \sim \frac{(1-\theta)6}{\pi^2 P \log P}.$$

Proof. Subtract (7) to obtain $h_P - h = \delta_P - (\rho - \rho_P)$ and apply Theorem 7.1. The strict inequality $\theta < 1$ follows from $B_1 < 1$. Expanding the positive product in (3) gives $\delta_P \sim (6/\pi^2)\sum_{p>P} p^{-2}$. By the prime number theorem and partial summation, $\sum_{p>P} p^{-2} = -\pi(P)/P^2 + 2\int_P^\infty \pi(t)t^{-3}\,dt \sim 1/(P\log P)$, with $\pi(t)$ the prime counting function. □

The conditional theorem uses a named external preprint. The deterministic conclusions arise from finite spatial-pattern frequencies, not from asserting a typical origin or independent bonds. Neither existence of h nor the bounds in the next section rely on it. The companion technical supplement contains the finite-pattern details and numerical certificates for the present planar model only. The odd–even equality also rules out a single linear second-order term ck in $\beta_1(K_k) = hk^2/2 + ck + o(k)$: consecutive even–odd differences would be $hk + o(k)$ instead of zero.

8. Exact computations and certified bounds

The accompanying C++17 programs compare direct deleted-site counts, the reduced graph, and Euler counts. A lifted quotient traversal detects torus winding; independent union–find counts check the quotient component and edge totals. Tables 1 and 2 report the retained exact data from the earlier computations. The numerical certificates use these integer data, not a fit to the finite observations.

Table 1. Direct and reduced counts at selected even levels. Here $r(G_m)$ is the cycle rank of the coarse graph, including boundary components.

$k = 2m$	n_k	$\beta_1(K_k)$	$r(G_m)$	β_1/n_k
50	1,326	131	2	.098793
100	5,151	517	10	.100369
200	20,301	2,192	40	.107975
500	125,751	13,604	188	.108182
1,000	501,501	54,417	616	.108508
2,000	2,003,001	218,256	2,468	.108964
4,000	8,006,001	872,199	10,136	.108943
8,000	32,012,001	3,492,812	40,226	.109109
22,000	242,033,001	26,416,327	303,174	.109143

Table 2. Periodic sieve counts. $M = M_P$, E counts quotient edges, F counts components with finite lifts. The listed cases have no winding components.

P	M	M^2	E	F	ρ_P
3	3	9	3	6	0
5	15	225	99	126	0
7	105	11,025	5,427	5,610	.000272109
11	1,155	1,334,025	684,315	652,206	.000467757
13	15,015	225,450,225	118,966,995	107,057,562	.000636872

At $P = 13$, Lemma 3.1 and Corollary 3.3 give the exact rational value

$$\rho_{13} = \frac{118966995 - 225450225 + 107057562}{4 \cdot 15015^2} = \frac{4351}{6831825}.$$

In particular the cycle rank of the quotient (with all lifts finite) is 574332. The inequality of Theorem 6.3 further sharpens the matching bound without requiring any larger periodic enumeration. The $k = 22000$ finite calculation gives $\beta_1/k^2 \approx 0.0545791880$; it is not itself a bound on the limit.

Corollary 8.1 (Computer-assisted numerical enclosure)**.** *The finite enumerations and rational certificates specified below give*

$$\boxed{0.10917978 < h < 0.10923225.} \tag{11}$$

Consequently $0.05458989 < \lim_{k\to\infty} \beta_1(K_k)/k^2 < 0.054616125$.

Proof. The following finite computation is part of the certificate, rather than a purely analytic evaluation of the constant. The detailed algorithms and exact outward-rounding inequalities are in the companion supplement and source files.

Lower endpoint. A visible island of shape A is characterized by visibility on A and deletion on its non-even neighboring boundary B. Enumerate normalized even-translation shapes through ten sites and sum the disjoint pattern frequencies, dividing by four. At a finite cutoff $R = 10000$, compute the probability of each event by covering the boundary with independent CRT residue choices, avoiding the $a = |A|$ visible sites. For small primes use a mask of covered boundary points; above the coordinate span, all offsets are distinct and the state is just the count j of still-uncovered boundary points. With F_j the completion probability for the remaining primes, the backward transition for a new prime is

$$F_j \leftarrow (1 - (a + j)/p^2)F_j + (j/p^2)F_{j-1},$$

where the second term is zero for $j = 0$. The terminal values are $F_0 = 1, F_{j>0} = 0$. All terms are nonnegative for feasible states. Outward integer rounding and a union bound for survival of A under omitted primes give $b_0 > 0.00017854739$. The local Euler term has the certified lower bound $-\bar{\chi} > 0.10900123267$, from Euler products with explicit tails and Machin arctangent bounds. Their exact rational sum exceeds 0.10917978. The positive recurrence in `island_positive.py` is an alternative to the signed symmetric inclusion–exclusion in `island_certificate.py`; the older dual-face certificate through eight triangles gives $h > 0.10917927$ by a separate geometric enumeration. The site procedures share shape generation and local arithmetic but not the large-prime probability recurrence.

Upper endpoint. At each near prime $13 < q \le 97$ use Theorem 6.4 with $L_q = 5$; beyond 97 use $B_5 < 0.083806377$. For example $b_5(S_{<17}) < 0.054400754$, compared with the full-sieve bound 0.083806377. The finite component-pattern sums are computed with the exact residue signatures of the forced-absent edges in inclusion–exclusion; the omitted-prime error for the full test is bounded by $238\tau_R$ with $\tau_R \ge \sum_{p>R}(p^2 - 1)^{-1}$ (see supplement). This yields $h < 0.10923686$ without a larger quotient than 15015.

At $q = 17$, `prefix_diameter.cpp` counts exactly 557383680 absent bonds in the period $M = 15015$, of which 29121696 are chords. Its winding-aware traversal verifies that no absent nonchord joins two lifted components both of diameter greater than 7. Proposition 6.5 therefore gives the exact increment

$$\Delta\rho_{17} = \frac{29121696}{4 \cdot 15015^2 \cdot 17^2}.$$

Use this instead of the corresponding near-prime upper term. For $z = 6/\pi^2$, the remaining tail expression $z - 1/2 + \rho_{13} + \Delta\rho_{17} + \sum_{17<q\le 97} b_5(S_{<q})\Delta e_q + B_5(3Q_1(97)/4 - z)$ is increasing in z because $B_5 < 1$. The exact arithmetic in `stratified_certificate.py` and `stratified_check.py` certifies the displayed strict upper endpoint. The latter checks saved rational values only; full enumeration is the former program. No period of order M_{17}^2 is traversed. Dividing the enclosure by two gives the last assertion. □

The origin-anchored triangular counts in Table 1 exhibit substantial finite-boundary and arithmetic sampling effects and do not imply monotonicity or one-sided convergence. A supplementary direct site enumeration in 3000×3000 boxes gives interior island counts $1724, 1633, 1578, 1616$ at lower-left corners $(0, 0), (10^7, 3 \cdot 10^7), (31415926535, 27182818284), (100000003, 700000001)$, respectively. With the local Euler term these give descriptive estimates near 0.10918; the boxes are deterministic, not unbiased random samples or confidence intervals. The rigorously certified lower endpoint is close to these observations, but an exponentially small island-size tail is not proved. The upper endpoint is still farther from these observations than the lower endpoint, but the stratified sieve reduces the previous discrepancy.

9. An independent chord lower bound and prime interactions

For an odd prime $q > 13$, let $S_{<q}$ denote the sieve of odd primes strictly below q, and let e be one distinguished coarse-lattice bond. Write

$$\vartheta(S_{<q}) = \Pr\big(u \leftrightarrow v \text{ in } G^{(S_{<q})} \,\big|\, e = uv \text{ absent}\big).$$

Here $u \leftrightarrow v$ means connection in the *old* graph with e absent, and all probabilities are the finite-pattern CRT frequencies. For each $\ell \geq 2$, let $\alpha_\ell(S_{<q})$ be the corresponding probability that a connecting path of length at most ℓ exists. Thus $0 \leq \alpha_\ell(S_{<q}) \leq \vartheta(S_{<q})$, and $\alpha_\ell(S_{<q})$ is nondecreasing as primes are adjoined.

Proposition 9.1 (Chord/nonchord decomposition)**.** *For each odd prime q the cycle-density increment admits the exact decomposition*

$$\Delta\rho_q = \vartheta(S_{<q})\,\Delta e_q + N_q, \qquad N_q \geq 0.$$

The first summand counts bonds added by q whose endpoints were already connected in the old graph. The nonnegative remainder N_q is the cycle rank density of the nonloop edges of the contracted multigraph of old components. In particular,

$$\Delta\rho_q \geq \alpha_\ell(S_{<q})\Delta e_q.$$

Proof. Work first in a finite induced triangle, and contract every connected component of the old sieve to a vertex. An added bond becomes a loop precisely when its endpoints are connected in the old graph. Every such loop raises $E - V + c$ by one, regardless of the order in which the new bonds are added. Removing the loops leaves a multigraph, whose cycle rank is nonnegative; this is the remaining increment. Boundary terms vanish after division by the number of fine vertices, while the finite old sieve makes the relevant connection probability and new-prime activation independent by CRT. This yields the displayed decomposition in the spatial limit. A short connecting path is a sufficient condition for a chord, proving the lower bound. □

Proposition 9.2 (A selected length-six finite-path certificate)**.** *A second positive CRT computation, using selected alternative paths of length at most six and not using the island-shape enumerator, certifies*

$$\boxed{h > 0.10914952.}$$

This is strictly stronger than the earlier length-three chord certificate but weaker than the island-based lower endpoint of Corollary 8.1.

Proof. Fix the coarse bond between $(0,0)$ and $(1,0)$. All simple paths avoiding that bond and of length at most six form a finite list of 144 paths. We deliberately use only a reproducible *subset* of 23 of these paths, supported on 18 candidate bonds including the target. The subset is generated deterministically from paths of length at most three, then enlarged by all paths already supported and by a lexicographically selected sequence of paths subject to a 19-bond cap. Every selected path has length at most six. This is a sufficient event for connection, not the full event α_6.

For each odd prime p, the randomly translated forbidden residue modulo p activates the selected bonds with the corresponding midpoint residue. Conditional on the target bond being absent, the residue excludes exactly one class out of p^2; the integer transition counts of activated-bond masks therefore have denominator $p^2 - 1$. Midpoint collisions modulo small primes are retained without an independence assumption. Let $\widehat{\alpha}_6(S)$ be the resulting exact conditional probability that at least one of the 23 selected paths is active, using primes in S. Then $0 \leq \widehat{\alpha}_6(S) \leq \alpha_6(S) \leq \vartheta(S)$, and $\widehat{\alpha}_6$ is monotone under adding primes.

At $q = 17$ we retain the exact independently counted increment $\Delta\rho_{17}$ of Proposition 6.5. For $19 \leq q \leq 97$ replace $\alpha_3(S_{<q})$ in the previous finite-prime chord inequality by $\widehat{\alpha}_6(S_{<q})$, and use $\max\{\widehat{\alpha}_6(S_{<101}), \vartheta(S_{<17})\}$ for the remaining edge density δ_{97}. This yields

$$\begin{aligned} h \geq \frac{6}{\pi^2} - \frac{1}{2} + \rho_{13} + \Delta\rho_{17} \\ + \sum_{\substack{19 \leq q \leq 97 \\ q \text{ prime}}} \max\{\widehat{\alpha}_6(S_{<q}), \vartheta(S_{<17})\}\,\Delta e_q \\ + \max\{\widehat{\alpha}_6(S_{<101}), \vartheta(S_{<17})\}\,\delta_{97}. \end{aligned}$$

The outward rational calculation in `chord_path6.py` exceeds the displayed strict decimal endpoint. A separate C++ implementation, `check_chord_path6.cpp`, performs direct residue translations and bounded-length graph search; its counts on complete periods 15, 105 and 1155 agree exactly with the mask recurrence. The code supplies the 23 paths explicitly. As a deliberately smaller sufficient event, this certificate does *not* reproduce the sharp island-based endpoint, and we do not claim that it does. □

Remark 9.3 (A conjecture, not an estimate). The exact decomposition isolates the unknown cross-component contribution N_q. At $q = 17$ the finite-period chord criterion proves $N_{17} = 0$. Numerical evidence suggests the total later nonchord contribution may be small, but no upper bound of order 10^{-6} is proved. We make *no numerical*

claim for $\sum_{q>17} N_q$ in the statements of this article. The chord series alone is not asserted to equal the complete cycle density.

Remark 9.4 (Order-free prime interactions). For any *finite* set S of odd primes, Boolean-lattice Möbius inversion gives the canonical coefficients

$$I(T) = \sum_{U \subseteq T} (-1)^{|T|-|U|} \rho(U), \quad \rho(S) = \sum_{T \subseteq S} I(T).$$

Since the one- and two-prime graphs are forests, $I(T) = 0$ for $|T| \leq 2$. The first possibly nonzero interactions have order three. For example, $I(\{3,5,7\}) = \rho(\{3,5,7\}) = 12/44100 = 1/3675$; this value can be obtained from the period-105 quotient and the one- and two-prime forest theorem. This is an exact finite combinatorial transform, not a claim of convergence of an infinite Dirichlet series or of a new general Möbius-inversion theorem. It is a natural starting point for studying order-independent prime interactions.

10. Relation to the literature and further questions

Baake, Moody and Pleasants [3, Proposition 4 and Theorem 3] prove positive-density arbitrarily large vacant regions and determine diffraction of visible lattice points. Pleasants and Huck [4, Section 3, Theorem 1] give the mixed finite-pattern frequency formula. The Euler products used here, including $Z(L)$, are applications of that formula restricted to the even translation class (the odd-prime CRT calculation gives the restriction directly). They are not proposed as new general arithmetic frequency identities.

Le Fourn, Liu and Martineau [5, Theorems 1.6–1.7, Sections 5.2–5.3 and 5.6.1] explicitly treat the triangular and D_d lattices with minimal-vector Cayley adjacency. In the random coprime coloring they prove an almost surely unique infinite visible cluster and, for these lattices, no infinite nonvisible cluster. Their result concerns a stationary random translate model; we do not infer the corresponding deterministic assertion for the fixed origin solely from an almost-sure statement. Our normalized counts require no such assertion and concern finite components, not the number of infinite clusters.

Cellarosi [6, Definitions 1.1–1.3, Proposition 2.4] studies non-r-free points on the cubical nearest-neighbor graph (four neighbors in dimension two). His component representatives belong to finite components containing an R-deep point; the size truncation in Proposition 2.4 has remainder at most $1/(L+1)$. That technique applies with our different adjacency and without a depth condition. His Theorem 1.7 and Corollary 1.8 concern large-R logarithmic density asymptotics, not Betti densities or midpoint cycle rank. We claim no originality for the general finite-pattern or bounded-size approximation machinery.

Our specific structural results are the midpoint and island correspondences, prime matchings and forests, diameter exclusion and stratified cycle bounds. Proposition 9.1 makes explicit the positive chord/nonchord decomposition, and Proposition 9.2 provides a structurally separate, albeit numerically weaker, length-six lower certificate. Full global priority is not established. Using only full-graph B_L has an intrinsic floor $B_L \geq \theta$ at fixed cutoff; an observed decimal plateau is not itself a certified barrier. The stratified theorem avoids that loss. Remaining questions include exponential island tails, exact evaluation of h, quantitative prime-increment convergence, and parity-specific second-order expansions.

Extensions to higher-dimensional lattices require separate constructions and are outside the scope of this planar preprint.

Reproducibility and status

The companion technical supplement specifies the enumeration, finite-pattern probabilities, rational rounding, and boundary conventions. The selected length-six chord-only certificate is not independent numerical corroboration of the sharp island endpoint: its rigorous value 0.10914952 remains lower than the island bound 0.10917978. Improvements at component-size cutoffs $L = 6, 7, 8$ for the earliest primes remain uncompleted and are not included in the certified enclosure. The code and recorded data are supplied with this preprint. Run the full certificates, not just the saved-number checks, to reproduce the numerical enclosure. The numerical statements are computer-assisted, and their implementation is not formally verified in a proof assistant. The other main results are analytic; the prime-increment law and its rate corollary are expressly dependent on the stated external nonpercolation result. All finite-window measurements are descriptive, not statistical confidence intervals. A permanent code link can be added to the public repository record when the companion files are deposited. The corrected saved-certificate checker reads but never writes its input data; a complete replay of the expensive signature generator is recorded in the accompanying reproducibility archive.

AI-assistance disclosure. This manuscript was developed with substantial generative-AI assistance from ChatGPT (OpenAI), Claude (Anthropic), Gemini (Google), and Copilot (Microsoft) in conjecture generation, proof formulation and development, computational design and execution, criticism, literature exploration and writing. The text and code are substantially AI-assisted; the systems are not authors or human referees. The author is responsible for reviewing, understanding, verifying and approving the entire work before dissemination. No human peer review, formal verification, or exhaustive priority determination is claimed.

References

[1] S. N. Jihad, *The Generative Arithmetic Fabric: A Unified Geometric Workbench for Arithmetic and Generator Deformation*, preprint v2.1, October 2026, Zenodo. https://doi.org/10.5281/zenodo.23126296.

[2] M. Kahle, *Topology of random simplicial complexes: a survey*, Contemporary Mathematics **620** (2014), 201–222. https://arxiv.org/abs/1301.7165v2.

[3] M. Baake, R. V. Moody and P. A. B. Pleasants, *Diffraction from visible lattice points and k-th power free integers*, Discrete Math. **221** (2000), 3–42. https://arxiv.org/abs/math/9906132v2.

[4] P. A. B. Pleasants and C. Huck, *Entropy and diffraction of the k-free points in n-dimensional lattices*, Discrete Comput. Geom. **50** (2013), 39–68. https://arxiv.org/abs/1112.1629v3.

[5] S. Le Fourn, M. Liu and S. Martineau, *Percolative properties of the random coprime colouring*, preprint (2025), arXiv:2509.08452v1. https://arxiv.org/abs/2509.08452v1.

[6] F. Cellarosi, *Density of large holes among power-free lattice points*, preprint (2026), arXiv:2609.25457v2. https://arxiv.org/abs/2609.25457v2.

[7] A. Hatcher, *Algebraic Topology*, Cambridge University Press, 2002, Section 3.3, Corollary 3.45, p. 255. https://pi.math.cornell.edu/~hatcher/AT/ATpage.html.

Independent Researcher, Iraq
Email address: sabahnoorij@gmail.com